Exploring the synthesis of key superheavy nuclei using ^{40}Ar as the projectile[*]

Jia-Xing Li[1] and Hong-Fei Zhang[1,2,†]

[1] *School of Physics, Xi'an Jiaotong University, 710049 Xi'an, People's Republic of China*

[2] *School of Nuclear Science and Technology, Lanzhou University, 730000 Lanzhou, People's Republic of China*

The study provides a comprehensive analysis of all stages of the heavy-ion fusion evaporation reaction, aiming to enhance the understanding of the entire process and identify the influencing factors in calculating the evaporation residue cross section. By focusing on the synthesis of superheavy nuclei with $Z = 114$, we discuss the capture cross section, fusion probability, and survival probability of the ^{48}Ca $+^{244}$ Pu reaction, and we compare them with those of the ^{40}Ar $+^{248}$ Cm reaction. Moreover, a systematic study examines the evaporation residue cross sections for the synthesis of superheavy nuclei with $Z = 112 - 116$ using ^{40}Ar as the projectile nucleus. The research indicates that utilizing ^{40}Ar as the projectile nucleus for synthesizing isotopes with $Z = 114$ offers advantages such as lower incident energy and reduced experimental costs. Furthermore, using ^{40}Ar as the projectile nucleus promises the synthesis of the new key isotope ^{285}115, thereby aiding in the identification of the new element.

Keywords: Superheavy nuclei, Dinuclear system model, Heavy-ion fusion

I. INTRODUCTION

The synthesis of superheavy nuclei (SHN) is one of the forefront research topics in modern nuclear physics. Using ^{48}Ca beams and actinide targets, hot fusion reactions in the neutron evaporation channels have successfully synthesized SHN with charge numbers $Z = 112 - 118$ [1–7]. Most microscopic-macroscopic models propose that element Fl ($Z = 114$) possesses a closed proton shell [8–11]. Recent research data from Ref. [12] once again underscores the significance of proton shell closures for nucleus Fl. The first synthesis of Fl isotopes occurs in 1999 by the Dubna group through the reaction ^{48}Ca $+^{244}$ Pu at the Dubna gas filled recoil separator (DGFRS). Two decay chains are observed, with the identification of ^{288}Fl and ^{289}Fl [13]. Subsequently, using higher projectile energies, the isotope ^{287}Fl is observed at an excitation energy of $E^* = 53$ MeV, with a corresponding maximum production cross section of $1.1^{+2.6}_{-0.9}$ pb [14]. Later, other isotopes are also obtained in reactions ^{48}Ca $+^{242}$ Pu, ^{48}Ca $+^{240}$ Pu and ^{48}Ca $+^{239}$ Pu [15–17]. Notably, recent investigations of the ^{48}Ca $+^{242}$ Pu reaction have provided valuable data, contributing to constraining theoretical predictions [12, 18]. However, based on the current experimental data, the structural properties of the Fl isotope chain are not well understood, thus requiring a substantial amount of additional experimental data. In this letter, the investigation of new methods for synthesizing Fl isotopes appears to be highly significant.

The synthesis of new element $Z = 119$ and the exploration of the limits of element existence pose challenging tasks [19–23]. Recently, the reaction ^{54}Cr $+^{243}$ Am has been proposed as the most promising method for synthesizing the new element [24–26]. α-decay is an important decay mode for SHN [27–29]. Experimentally, the identification of new elements and isotopes can be achieved by observing the position-time correlated α-decay chains from an unknown parent nucleus to its known descendants [30–32]. Studying the isotopes along the α-decay chain of a new element is crucial for its identification. However, as illustrated in Fig. 1, there are undiscovered nuclides along the α-decay chain of the predicted synthesized nuclide ^{293,294}119. Thus, this paper proposes the utilization of ^{40}Ar as the projectile nucleus. This approach holds promise for synthesizing new nuclides along the alpha α-decay chain of the new element, thereby facilitating its identification.

In heavy-ion fusion reactions, the entire process of compound nucleus formation and decay is typically divided into three stages: the capture process where the colliding system overcomes the Coulomb barrier, the formation of the compound nucleus by surpassing the inner fusion barrier, and the de-excitation of the excited compound nucleus to counter fission. The evaporation residue cross section is expressed as a sum over partial waves with angular momentum J at the center-of-mass energy $E_{c.m.}$ [33–35],

$$\sigma_{ER}\left(E_{c.m.}\right) = \frac{\pi\hbar^2}{2\mu E_{c.m.}} \sum_{J=0}^{J_{\max}} (2J+1)\, T\left(E_{c.m.}, J\right) \times P_{\text{CN}}\left(E_{c.m.}, J\right) \times W_{\text{sur}}\left(E_{c.m.}, J\right). \tag{1}$$

Here, the transmission probability $T(E_{c.m.}, J)$ is affected by the Coulomb barrier and strong channel coupling with internal degrees of freedom. This coupling significantly enhances the capture cross section by several orders of magnitude at sub-barrier energies [36]. When the capture cross section is experimentally measured within a near-barrier energy range, the barrier height and the barrier distribution function can be derived from the experimental data. Subsequently, the $T(E_{c.m.}, J)$ can be readily calculated or approximated. However, in the synthesis of superheavy elements, measuring the capture cross section directly is challenging and is typically inferred from the total yield of fission fragments. In such cases, the $T(E_{c.m.}, J)$ needs to be estimated using theoretical models that describe the initial stages of the reaction. P_{CN} is the fusion probability. The fusion stage of the re-

[*] Helpful discussions with Zai-Guo Gan and Zhi-Yuan Zhang are gratefully acknowledged. This work is supported by the National Natural Science Foundation of China (Grants No. 12175170 and 11675066).

[†] Corresponding author, zhanghf@xjtu.edu.cn

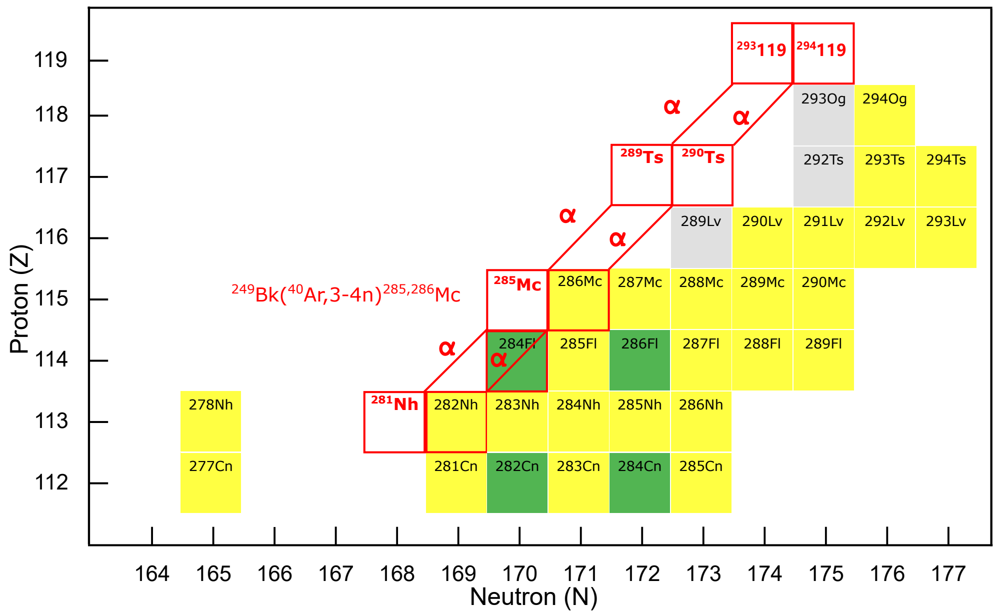

Fig. 1. The α decay chain of the new element with $Z = 119$. The filled squares and open squares denote the known nuclei and the predicted ones, respectively. Yellow and olive indicate the α decay and spontaneous fission, respectively. Gray represents unknown decay modes.

action is relatively less studied. This is because in light and medium nucleus fusion, the fissility of the compound nucleus is low, and the probability of forming a compound nucleus after overcoming the Coulomb barrier is close to 1 ($P_{CN} \approx 1$). However, in heavy nucleus fusion, the heavy system may reseparate into two fragments without forming a compound nucleus (quasifission). Thus, the value of P_{CN} may be far less than 1, and accurate calculation of P_{CN} is challenging. The formation dynamics of SHN in massive fusion and multinucleon transfer reactions are intricate, involving the interplay of numerous degrees of freedom including radial elongation, mass or charge asymmetry, shape configuration, relative motion energy, and more [37–40]. To describe the fusion hindrance in massive systems, several models have been developed, including macroscopic dynamical models [41], fusion-by-diffusion models [42], dynamical models based on Langevin-type equations [43], and dinuclear system (DNS) models [44–46]. Today there is no consensus for the mechanism of the compound nucleus formation itself, and quite different, sometimes opposite in their physics sense, models are used for its description. W_{sur} is the survival probability, typically calculated using statistical models. In the calculation of the W_{sur}, the fission barrier of the excited compound nucleus is the most important and ambiguous parameter, as theoretical estimates of the fission barrier in the SHN region are not yet very reliable and exhibit significant differences among them [47].

Our aim is to theoretically analyze three stages of fusion reactions to understand the factors influencing evaporation residue cross sections at each stage, and to explore the possibility of synthesizing key new isotopes using ^{40}Ar as the projectile nucleus. In Sec. II, we introduce the theoretical framework. In Sec. III, we analyze and discuss the results. In Sec. IV, we summarize our work.

II. THEORETICAL DESCRIPTIONS

The most widely used method for calculating capture cross section is the coupled-channel approach. The computer code CCFULL, which is based on the coupled-channel formalism, is utilized to perform these calculations (for a detailed description, see Ref. [48]). This involves numerically solving the following set of coupled-channel equations:

$$\left[-\frac{\hbar^2}{2\mu}\frac{d^2}{dr^2} + \frac{J(J+1)\hbar^2}{2\mu r^2} + V_N^{(0)}(r) + \frac{Z_P Z_T e^2}{r} + \epsilon_n - E\right] \psi_n(r) \quad + \sum_m V_{nm}(r)\psi_m(r) = 0, \tag{2}$$

where r represents the radial part of the relative motion coordinate and μ stands for the reduced mass. The bombarding energy in the center of mass frame is denoted by E, and ϵ_n signifies the excitation energy of the n-th channel. The elements V_{nm} are matrix components of the coupling Hamiltonian, which in the collective model include both Coulomb and nuclear terms. These components are elaborated in the subsequent section. $V_N^{(0)}$ is the nuclear potential in the entrance channel.

However, for SHN, an empirical coupled-channel (ECC) method is typically used when calculating the capture cross section of SHN [49]. In this method the transmission probability $T(E_{\text{c.m.}}, J)$ can be calculated through the well-known Hill-Wheeler formula [50], which approximates the radial variation of the Coulomb barrier between colliding nuclei with a parabolic form. Taking into account now the multidi-

mensional character of the realistic barrier, we may introduce the barrier distribution function $f(B)$ in order to determine its total transmission probability [51],

$$T\left(E_{c.m.}, J\right) = \int f\left(B\right) \times \frac{1}{1+\exp\left(\frac{2\pi}{\hbar\omega(l)}\left[B+\frac{\hbar^2}{2\mu R_B^2(l)}l\left(l+1\right)-E\right]\right)}dB. \quad (3)$$

In this context, $\hbar\omega_B$ indicates the width of the parabolic barrier, while R_B defines the position of the barrier. $f(B)$ represents the empirical dynamical barrier distribution function, which, under Gaussian approximation, can be expressed as

$$f\left(B\right) = \begin{cases} \frac{1}{N}\exp\left[-\left(\frac{B-B_m}{\Delta_1}\right)^2\right] & B < B_m \\ \frac{1}{N}\exp\left[-\left(\frac{B-B_m}{\Delta_2}\right)^2\right] & B > B_m, \end{cases} \quad (4)$$

here, $B_m = \frac{B_s+B_0}{2}$, B_0 is the height of the Coulomb barrier at waist-to-waist orientation, and B_s is the minimum height of the Coulomb barrier with variance of dynamical deformation, N is the normalization constant. $\Delta_2 = \left(B_0 - B_s\right)/2$, The value of Δ_1 is usually 2-4 MeV less than the value of Δ_2.

In the framework of the DNS model, the P_{CN} is obtained by numerically solving a set of master equations, where the neutron and proton numbers of the projectile-like fragment are considered as variables, along with the corresponding potential energy surface variables [52]. The time evolution of the distribution probability function, $P(Z_1, N_1, E_1, t)$, which describes the probability at time t of finding Z_1 protons and N_1 neutrons in fragment 1 with excitation energy E_1, is obtained by the following master equation:

$$\begin{aligned} &\frac{dP(Z_1,N_1,E_1,t)}{dt} = \\ &\sum_{Z'_1} W_{Z_1,N_1;Z'_1,N_1}(t) \times [d_{Z_1,N_1}P(Z'_1,N_1,E_1,t) \\ &- d_{Z'_1,N_1}P(Z_1,N_1,E_1,t)] \\ &+ \sum_{N'_1} W_{Z_1,N_1;Z_1,N'_1}(t) \times [d_{Z_1,N_1}P(Z_1,N'_1,E_1,t) \\ &- d_{Z_1,N'_1}P(Z_1,N_1,E_1,t)] \\ &- \left\{\Lambda^{qf}\left[\Theta\left(t\right)\right] + \Lambda^{fs}\left[\Theta\left(t\right)\right]\right\} P\left(Z_1,N_1,E_1,t\right). \end{aligned} \quad (5)$$

Here $W_{Z_1,N_1;Z'_1,N_1}$ is the mean transition probability from the channel (Z_1, N_1) to (Z'_1, N_1), while d_{N_1,Z_1} denotes the microscopic dimension corresponding to macroscopic state (Z_1, N_1). All the possible proton and neutron numbers of the fragment 1 is taken into the sum, but only one nucleon transfer is considered in the model $(N'_1 = N_1 \pm 1, Z'_1 = Z_1 \pm 1)$. The quasifission rate Λ^{qf} and Λ^{fs} fission rate are estimated with the one-dimensional Kramers formula.The potential energy surface of the DNS in fusion process is defined as :

$$\begin{aligned} U\left(Z_1,N_1,Z_2,N_2,R\right) &= E_B(Z_1,N_1) + E_B(Z_2,N_2) \\ &- E_B(Z_{CN},N_{CN}) + V_C\left(R\right) + V_N\left(R\right), \end{aligned} \quad (6)$$

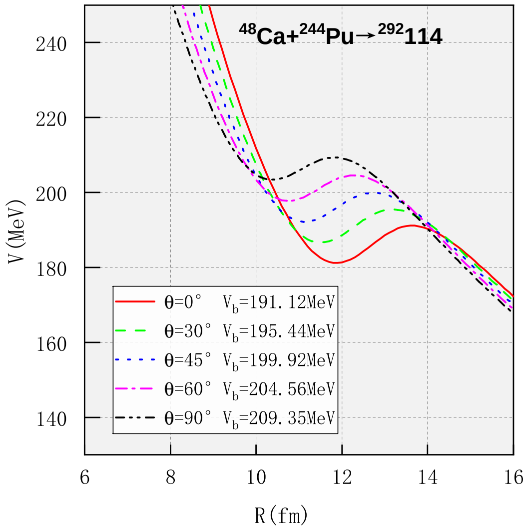

Fig. 2. Dependence of the nucleus-nucleus interaction potential on collision direction in the ^{48}Ca $+{}^{244}$ Pu reaction.

where $Z_{1,2}$ and $N_{1,2}$ are the proton numbers and neutron numbers of two fragments, respectively. $E_B(Z_i, N_i)$ and $E_B(Z_{CN}, N_{CN})$ are the binding energy of the fragment (Z_i, N_i) and the compound nucleus, respectively. We take the Coulomb potential $V_C\left(R\right)$ and nuclear potential $V_N\left(R\right)$ mentioned in Ref. [53]. The W_{sur} is calculated using a statistical model,

$$W_{sur}\left(E_{c.m.}, x, J\right) = P\left(E^*_{CN}, x, J\right)\prod_{i=1}^{x}\left[\frac{\Gamma_n}{\Gamma_n + \Gamma_f}\right]_i, \quad (7)$$

here, E^*_{CN} represents the excitation energy of the compound nuclei. $P\left(E^*_{CN}, x, J\right)$ is the realization probability of emitting x neutrons. Γ_n and Γ_f represent the partial wave decay width of evaporating neutron and fission respectively.

III. RESULTS AND DISCUSSION

In Fig. 2, we show the dependence of the barrier height on the collision orientation with static deformation in the ^{48}Ca $+{}^{244}$ Pu reaction. The quadrupole deformation parameter is taken from Ref. [57]. Since ^{48}Ca is a spherical nucleus, we only vary the orientation θ of ^{244}Pu. One can see that the Coulomb barrier height differs by 18.23 MeV between pole-to-pole collisions ($\theta = 0°$) and waist-to-waist collisions ($\theta = 90°$). This indicates that the collision orientation has a significant impact on the capture cross section. In the synthesis of SHN, it is crucial to consider not only the static deformation of the nuclei but also the significant dynamic deformations caused by nucleus-nucleus interactions.

In Fig. 3, we present the capture cross sections and evaporation residue cross sections for three reactions involved in the synthesis of SHN. The position of V_0 represents the height of the Coulomb barrier in the waist-to-waist direction. The position of V_s represents the height of the minimum barrier

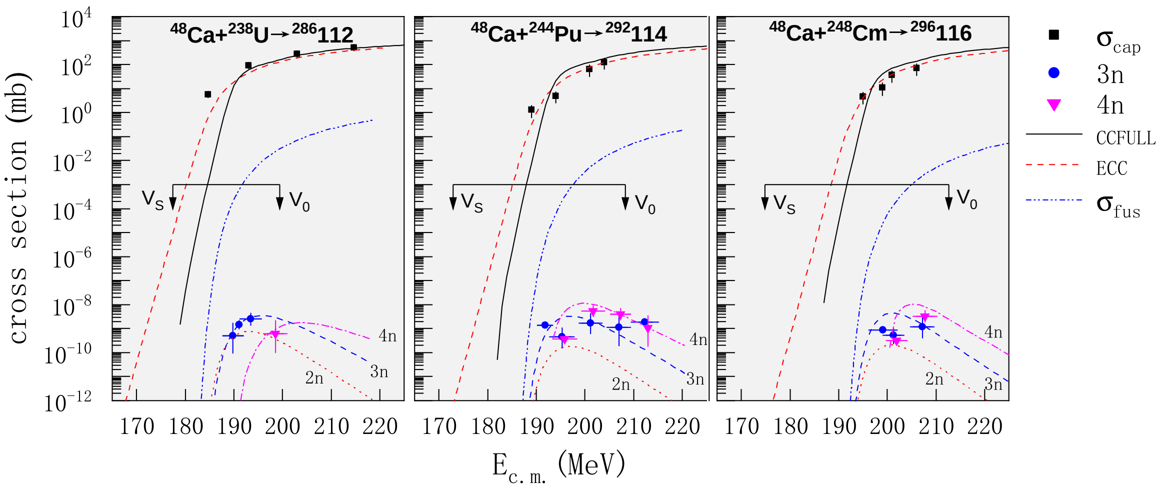

Fig. 3. Capture cross section σ_{cap}, fusion cross section σ_{fus} and evaporation residue cross sections in the $2n$, $3n$, and $4n$ channels. Experimental data for the capture cross section are taken from Ref. [54], and experimental data for the evaporation residue cross sections in the xn channels are taken from Ref. [14, 17, 55, 56]. Positions of the Coulomb barrier at waist-to-waist collision (V_0) and at the saddle point (V_S) are shown by the arrows.

that changes with dynamic deformation (the position of the Coulomb barrier at the saddle point). It can be seen that the difference $V_0 - V_s$ becomes greater and greater with increasing the masses of the interacting nuclei. We can also observe that the ECC model, compared to CCFULL, describes the capture cross sections of reactions for synthesizing SHN very well, including the sub-barrier energy region. This is because, for SHN (low-energy vibrational excitations), a realistic nucleus-nucleus interaction can lead to very large dynamic deformations. Thus, a large number of coupling channels need to be considered, which greatly complicates the microscopic calculation of $T(E_{c.m.}, J)$ and makes it unreliable. In this case, CCFULL calculations cannot reproduce the experimental capture cross sections at sub-barrier energies. Additionally, we have provided the fusion cross sections σ_{fus} ($\sigma_{\text{fus}} = \sigma_{\text{cap}} \times P_{\text{CN}}$) for these three reactions and calculated the evaporation residue cross sections. The results show that the calculated evaporation residue cross sections reproduce the experimental data very well.

Based on the theoretical description of SHN synthesis, we have conducted research on the synthesis of key superheavy isotopes. Figure. 4 shows the capture cross sections and evaporation residue cross sections for the $Z = 114$ isotope, which is predicted to have a proton magic number, synthesized using ^{40}Ar as the projectile nucleus. It can be seen that the maximum evaporation residue cross section of the reaction $^{40}\text{Ar} + ^{248}\text{Cm}$ appears in the $3n$ channel, with a maximum evaporation residue cross section of 4.6 pb, corresponding to an incident energy of 181.77 MeV. Additionally, the maximum evaporation residue cross section in the $4n$ channel closely matches that in the $3n$ channel, slightly below the maximum observed in the $3n$ channel. Experimental fusion reactions with ^{48}Ca as the projectile nucleus yield a maximum cross section of 5 pb for the synthesis of the $Z = 114$ isotope [14]. Thus, using ^{40}Ar as the projectile nucleus for

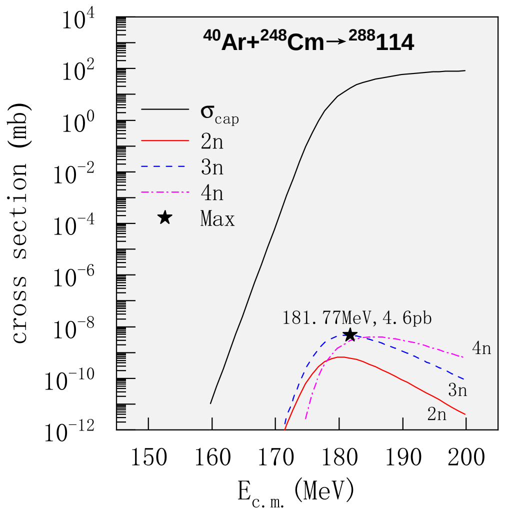

Fig. 4. Capture cross section σ_{cap} and evaporation residue cross sections in the $2n$, $3n$, and $4n$ channels in the $^{40}\text{Ar} + ^{248}\text{Cm}$ reaction. The maximum evaporation residue cross section is marked with a pentagram.

synthesizing the $Z = 114$ isotope not only has the advantages of reducing experimental costs and requiring lower incident energy, but the maximum evaporation residue cross section is also comparable to that induced by the ^{48}Ca fusion reaction.

To gain deeper insight into the physical mechanisms behind the synthesis of SHN using ^{40}Ar and ^{48}Ca, we analyze the P_{CN} using the DNS model. The advantage of the DNS model is that it can naturally explain the existence of an inner fusion barrier when forming a compound nucleus and includes the competitive processes of fusion and quasifission during the evolution of the dinuclear system towards the com-

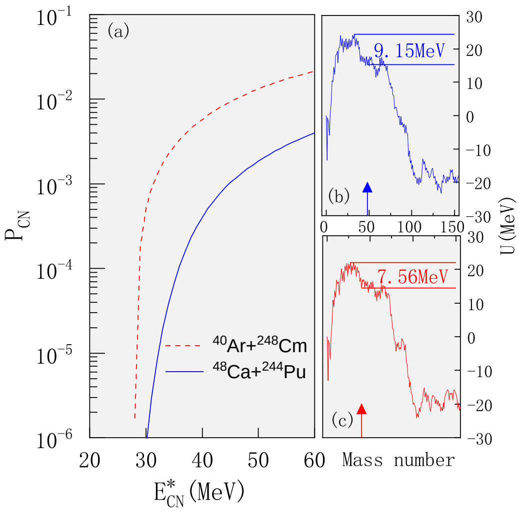

Fig. 5. (a) P_{CN} for ^{48}Ca $+^{244}$ Pu and ^{40}Ar $+^{248}$ Cm. (b) Driving potentials for the reaction ^{48}Ca $+^{244}$ Pu, with arrows indicating the entrance channel position. (c) Driving potentials for the reaction ^{40}Ar$+^{248}$ Cm, with arrows indicating the entrance channel position.

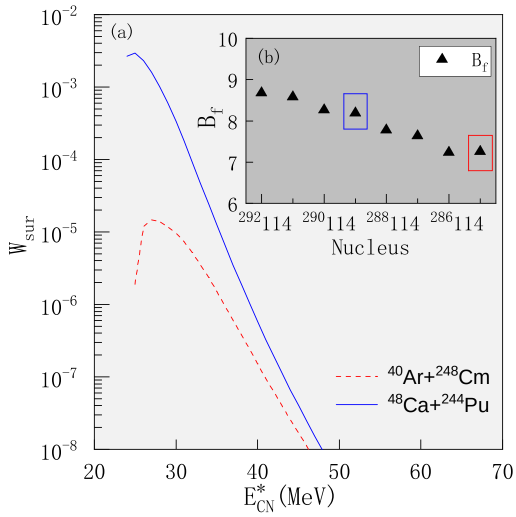

Fig. 6. (a) W_{sur} in the $3n$ channel for synthesizing a SHN with $Z = 114$ using the reaction systems ^{48}Ca$+^{244}$Pu and ^{40}Ar$+^{248}$Cm. (b) The fission barrier heights for the isotopic chain with $Z = 114$.

pound nucleus. In Fig. 5 (a), we show the P_{CN} for the synthesis of the $Z = 114$ isotope induced by ^{48}Ca and ^{40}Ar. It can be seen that the P_{CN} induced by ^{40}Ar is an order of magnitude higher than that induced by ^{48}Ca. Fig. 5 (b) and Fig. 5 (c) respectively show the driving potentials and inner fusion barrier heights of the reactions ^{48}Ca $+^{244}$ Pu and ^{40}Ar $+^{248}$ Cm. It can be seen that their inner fusion barrier heights are 9.15 MeV and 7.56 MeV, respectively. The larger the inner fusion barrier, the more difficult it is for the dinuclear system to evolve towards a compound nucleus. Conversely, the smaller the inner fusion barrier, the easier it is for the dinuclear system to evolve towards a compound nucleus. Thus, the reason for the higher P_{CN} of the reaction ^{40}Ar $+^{248}$ Cm is the greater mass asymmetry of the reaction system, resulting in a lower inner fusion barrier.

We also analyzed the W_{sur} in the 3n channel for the the aforementioned two reactions. In Fig. 6 (a), we can observe a higher W_{sur} for the ^{48}Ca $+^{244}$ Pu reaction system. For the reaction ^{48}Ca $+^{244}$ Pu, after the formation of the compound nucleus ^{292}114, three neutrons evaporate, resulting in nucleus ^{289}114. Similarly, for the reaction ^{40}Ar $+^{248}$ Cm, the compound nucleus ^{288}114 undergoes the evaporation of three neutrons, yielding nucleus ^{285}114. In other words, the $Z = 114$ isotope synthesized by the ^{48}Ca $+^{244}$ Pu reaction is relatively neutron-rich. In Fig. 6 (b), we illustrate the fission barrier heights along the $Z = 114$ isotope chain, marking the positions of nuclei ^{289}114 and ^{285}114. The fission barrier height difference between ^{289}114 and ^{285}114 is about 1 MeV. This 1 MeV difference in fission barrier height translates to roughly an order of magnitude difference in survival probabilities, hence the higher survival probability for the ^{48}Ca $+^{244}$ Pu reaction system.

The Ds isotopes in the reaction of ^{40}Ar $+^{238}$ U are measured by Dubna [58]. The cross section of the 5n evaporation

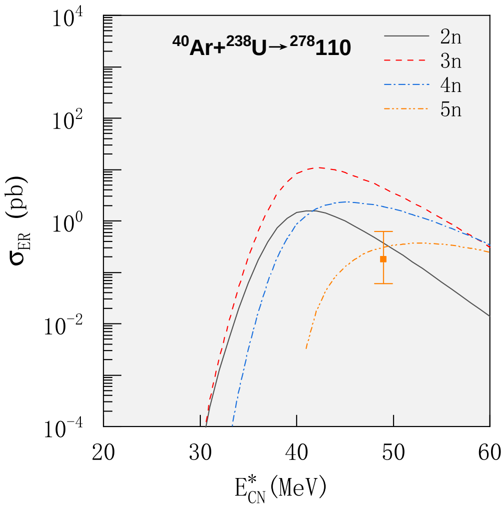

Fig. 7. The evaporation residue cross sections in the $2n$, $3n$, $4n$ and $5n$ channels for reaction ^{40}Ar $+^{238}$ U. Experimental data for the evaporation residue cross section in the $5n$ channel istaken from Ref. [58].

channel of the reaction at $E^* = 49$ MeV is $0.18^{+0.44}_{-0.12}$ pb. In Fig. 7, we show our calculation results for the 2n, 3n, 4n, and 5n evaporation channels. It can be seen that in the 5n evaporation channel, our results match the experimental data within the error range. Furthermore, it is noteworthy that our results show that the maximum cross section occurs in the 3n channel at this excitation energy. However, the measurement data for the 3n channel is not provided in Ref. [58], so it is necessary to conduct further experiments and obtain more experimental data to verify the reliability of the model.

In Fig. 8, we present the maximum evaporation residue cross sections for synthesizing SHN with $Z = 112 - 116$ us-

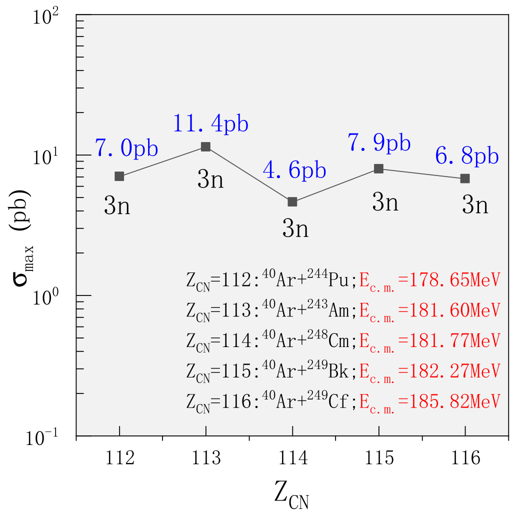

Fig. 8. The maximum evaporation residue cross sections for synthesizing SHN with $Z = 112 - 116$ using ^{40}Ar, along with the corresponding neutron evaporation channels and incident energies.

ing ^{40}Ar as the projectile nucleus, along with the corresponding neutron evaporation channels and incident energies. It can be observed that the maximum evaporation cross sections for these reactions occur in the 3n channel, and the maximum evaporation residue cross sections are all in the pb range. Such cross sections are similar in magnitude to those produced by fusion reactions induced by ^{48}Ca, suggesting the potential of using ^{40}Ar as a projectile nucleus for synthesizing SHN. Most importantly, the reaction ^{40}Ar $+^{249}$ Bk in the 3n channel can synthesize the crucial new isotope ^{286}115, which is part of the alpha decay chain of the new element $Z = 119$. The predicted maximum cross section for this reaction is 7.9 pb. Thus, before attempting to synthesize the new element $Z = 119$, it is recommended to experimentally synthesize ^{286}115 via the ^{40}Ar $+^{249}$ Bk reaction to facilitate the identification of the new element.

IV. SUMMARY

In summary, for the capture process, the ECC method effectively describes the experimental capture cross sections in the fusion reactions for synthesizing SHN, including the sub-barrier energy region. The dynamics of the fusion process remain unclear, and certain critical parameters in the survival process, such as the fission barrier height, are uncertain. This undoubtedly necessitates extensive experimental and theoretical research in the future. In this paper, we conducted a systematic study on the synthesis of SHN $Z = 112$ to $Z = 116$ using ^{40}Ar as the projectile, employing available experimental data and relatively accurate theoretical methods. The study indicates that ^{40}Ar can be used as a projectile to synthesize $Z = 114$ isotopes, allowing for the investigation of the stability of nuclei predicted to possess the proton magic number $Z = 114$. Additionally, ^{40}Ar can be used as a projectile to synthesize the key nucleus ^{286}115, which lies on the α-decay chain of the new element $Z = 119$, aiding in the identification of the new element. We hope that this paper provides valuable insights for future experiments using ^{40}Ar as a projectile to synthesize crucial superheavy nuclei.

[1] Y. Oganessian, Heaviest nuclei from 48Ca-induced reactions. J. Phys. G: Nucl. Part. Phys. **34**, R165 (2007). doi: 10.1088/0954-3899/34/4/R01

[2] Y. Ts. Oganessian, V. K. Utyonkov, Super-heavy element research. Rep. Prog. Phys. **78**, 036301 (2015). doi: 10.1088/0034-4885/78/3/036301

[3] Yu. Ts. Oganessian, F. Sh. Abdullin, P. D. Bailey, et al., Synthesis of a New Element with Atomic Number $Z = 117$. Phys. Rev. Lett. **104**, 142502 (2010). doi: 10.1103/PhysRevLett.104.142502

[4] S. Hofmann, S. Heinz, R. Mann, et al., Review of even element super-heavy nuclei and search for element 120. Eur. Phys. J. A **52**, 1–34 (2016). doi: 10.1140/epja/i2007-10373-x

[5] R. Eichler, N. V. Aksenov, A. V. Belozerov, et al., Chemical characterization of element 112. Nature **447**, 72–75 (2007). doi: 10.1038/nature05761

[6] L. Stavsetra, K. E. Gregorich, J. Dvorak, et al., Independent Verification of Element 114 Production in the ^{48}Ca $+^{242}$ Pu Reaction. Phys. Rev. Lett. **103**, 132502 (2009). doi: 10.1103/PhysRevLett.103.132502

[7] Ch. E. Düllmann, M. Schädel, A. Yakushev, et al., Production and Decay of Element 114: High Cross Sections and the New Nucleus ^{277}Hs. Phys. Rev. Lett. **104**, 252701 (2010). doi: 10.1103/PhysRevLett.104.252701

[8] P. Möller, A. J. Sierk, T. Ichikawa, et al., Nuclear ground-state masses and deformations: FRDM(2012). At. Data Nucl. Data Tables **109-110**, 1-204 (2016). doi: 10.1016/j.adt.2015.10.002

[9] A. Sobiczewski, K. Pomorski, Description of structure and properties of superheavy nuclei. Prog. Part. Nucl. Phys. **58**, 292-349 (2007). doi: 10.1016/j.ppnp.2006.05.001

[10] J. X. Li, W. X. Wang, H. F. Zhang, Properties and synthesis of the superheavy nucleus $^{298}_{114}$Fl. Phys. Rev. C **106**, 044601 (2022). doi: 10.1103/PhysRevC.106.044601

[11] M.-H. Zhang, Y. Zou, M.-C. Wang, et al., Possibility of reaching the predicted center of the island of stability via the radioactive beam-induced fusion reactions, Nuclear Science and Techniques **35**, 161 (2024). doi: 10.1007/s41365-024-01542-x.

[12] A. Såmark-Roth, D. M. Cox, D. Rudolph, et al., Spectroscopy along Flerovium Decay Chains: Discovery of ^{280}Ds and an Excited State in ^{282}Cn, Phys. Rev. Lett. **126**, 032503 (2021). doi: 10.1103/PhysRevLett.126.032503

[13] Yu. Ts. Oganessian, V. K. Utyonkov, Yu. V. Lobanov, et al., Synthesis of superheavy nuclei in the ^{48}Ca+^{244}Pu reaction: ^{288}114, Phys. Rev. C **62**, 041604 (2000). doi: 10.1103/PhysRevC.62.041604

[14] Yu. Ts. Oganessian, V. K. Utyonkov, Yu. V. Lobanov, et al., Measurements of cross sections for the fusion-evaporation reactions $^{244}\mathrm{Pu}(^{48}\mathrm{Ca}, xn)^{292-x}114$ and

^{245}Cm(^{48}Ca, xn)$^{293-x}$116, Phys. Rev. C **69**, 054607 (2004). doi: 10.1103/PhysRevC.69.054607

[15] P. A. Ellison, K. E. Gregorich, J. S. Berryman, et al., New Superheavy Element Isotopes: ^{242}Pu(^{48}Ca, $5n$)^{285}114, Phys. Rev. Lett. **105**, 182701 (2010). doi: 10.1103/PhysRevLett.105.182701

[16] V. K. Utyonkov, N. T. Brewer, Yu. Ts. Oganessian, et al., Experiments on the synthesis of superheavy nuclei ^{284}Fl and ^{285}Fl in the ^{239,240}Pu $+^{48}$ Ca reactions, Phys. Rev. C **92**, 034609 (2015). doi: 10.1103/PhysRevC.92.034609

[17] Yu. Ts. Oganessian, V. K. Utyonkov, Yu. V. Lobanov, et al., Measurements of cross sections and decay properties of the isotopes of elements 112, 114, and 116 produced in the fusion reactions ^{233,238}U, ^{242}Pu, and ^{248}Cm $+^{48}$ Ca, Phys. Rev. C **70**, 064609 (2004). doi: 10.1103/PhysRevC.70.064609

[18] Yu. Ts. Oganessian, V. K. Utyonkov, D. Ibadullayev, et al., Investigation of ^{48}Ca-induced reactions with ^{242}Pu and ^{238}U targets at the JINR Superheavy Element Factory, Phys. Rev. C **106**, 024612 (2022). doi: 10.1103/PhysRevC.106.024612.

[19] M.-H. Zhang, Y.-H. Zhang, Y. Zou, et al., Predictions of synthesizing elements with $Z = 119$ and 120 in fusion reactions, Phys. Rev. C **109**, 014622 (2024). doi: 10.1103/PhysRevC.109.014622

[20] G. G. Adamian, N. V. Antonenko, H. Lenske, et al., Predictions of identification and production of new superheavy nuclei with $Z = 119$ and 120, Phys. Rev. C **101**, 034301 (2020). doi: 10.1103/PhysRevC.101.034301

[21] F. Li, L. Zhu, Z.-H. Wu, et al., Predictions for the synthesis of superheavy elements $Z = 119$ and 120, Phys. Rev. C **98**, 014618 (2018). doi: 10.1103/PhysRevC.98.014618

[22] A. Nasirov, B. Kayumov, Optimal colliding energy for the synthesis of a superheavy element with $Z = 119$, Phys. Rev. C **109**, 024613 (2024). doi: 10.1103/PhysRevC.109.024613

[23] X.-Q. Deng, S.-G. Zhou, Examination of promising reactions with ^{241}Am and ^{244}Cm targets for the synthesis of new superheavy elements within the dinuclear system model with a dynamical potential energy surface, Phys. Rev. C **107**, 014616 (2023). doi: 10.1103/PhysRevC.107.014616

[24] Z. Wang, Z. Ren, Exploring α-decay chains and cluster radioactivities of superheavy 293-295 119 isotopes, Eur. Phys. J. A **60**, 74 (2024). doi: 10.1140/epja/s10050-024-01301-x

[25] B. M. Kayumov, O. K. Ganiev, A. K. Nasirov, et al., Analysis of the fusion mechanism in the synthesis of superheavy element 119 via the ^{54}Cr+ ^{243}Am reaction, Phys. Rev. C **105**, 014618 (2022). doi: 10.1103/PhysRevC.105.014618

[26] F. Niu, P.-H. Chen, Z.-Q. Feng, Systematics on production of superheavy nuclei Z= 119-122 in fusion-evaporation reactions, Nucl. Sci. Tech. **32**, 103 (2021). doi: 10.1007/s41365-021-00946-3

[27] W. M. Seif, A. R. Abdulghany, Stability and α decay of translead isomers and the related preformation probability of α particles, Phys. Rev. C **108**, 024308 (2023). doi: 10.1103/PhysRevC.108.024308

[28] K. Prathapan, P. Deneshan, M. K. Preethi Rajan, et al., A systematic study of alpha decay half-lives of isotopes in superheavy region, Indian J. Phys. **98**, 2121-2132 (2024). doi: 10.1007/s12648-023-02996-2

[29] B.-S. Cai, C.-X. Yuan, Random forest-based prediction of decay modes and half-lives of superheavy nuclei, Nuclear Science and Techniques **34**, 204 (2023). doi: 10.1007/s41365-023-01354-5.

[30] Z. Y. Zhang, H. B. Yang, M. H. Huang, et al., New α-Emitting Isotope ^{214}U and Abnormal Enhancement of α-Particle Clustering in Lightest Uranium Isotopes, Phys. Rev. Lett. **126**, 152502 (2021). doi: 10.1103/PhysRevLett.126.152502

[31] Z. Ren, B. Zhou, Alpha-clustering effects in heavy nuclei, Front. Phys. **13**, 132110 (2018). doi: 10.1007/s11467-018-0846-3

[32] S. A. Giuliani, Z. Matheson, W. Nazarewicz, et al., Colloquium: Superheavy elements: Oganesson and beyond, Rev. Mod. Phys. **91**, 011001 (2019). doi: 10.1103/RevModPhys.91.011001

[33] G. G. Adamian, N. V. Antonenko, W. Scheid, et al., Treatment of competition between complete fusion and quasifission in collisions of heavy nuclei, Nucl. Phys. A **627**, 361-378 (1997). doi: 10.1016/S0375-9474(97)00605-2

[34] G. G. Adamian, N. V. Antonenko, W. Scheid, et al., Fusion cross sections for superheavy nuclei in the dinuclear system concept, Nucl. Phys. A **633**, 409-420 (1998). doi: 10.1016/S0375-9474(98)00124-9

[35] G. Giardina, S. Hofmann, A. I. Muminov, et al., Effect of the entrance channel on the synthesis of superheavy elements, Eur. Phys. J. A **8**, 205-216 (2000). doi: 10.1007/s10050-000-4509-7

[36] M. Dasgupta, D. J. Hinde, N. Rowley, et al., Measuring barriers to fusion, Ann. Rev. Nucl. Part. Sci. **48**, 401-461 (1998). doi: 10.1146/annurev.nucl.48.1.401

[37] P. H. Chen, F. Niu, Y. F. Guo, Z. Q. Feng, Nuclear dynamics in multinucleon transfer reactions near Coulomb barrier energies, Nuclear Science and Techniques **29**, 185 (2018). doi: 10.1007/s41365-018-0521-y.

[38] C. Li, P. Wen, J. Li, G. Zhang, B. Li, F.-S. Zhang, Production of heavy neutron-rich nuclei with radioactive beams in multinucleon transfer reactions, Nuclear Science and Techniques **28**, 110 (2017). doi: 10.1007/s41365-017-0266-z.

[39] Z.-Q. Feng, Nuclear dynamics and particle production near threshold energies in heavy-ion collisions, Nuclear Science and Techniques **29**, 40 (2018). doi: 10.1007/s41365-018-0379-z.

[40] F. Niu, P.-H. Chen, H.-G. Cheng, et al., Multinucleon transfer dynamics in nearly symmetric nuclear reactions, Nuclear Science and Techniques **31**, 59 (2020). doi: 10.1007/s41365-020-00770-1.

[41] S. Bjørnholm, W. J. Swiatecki, Dynamical aspects of nucleus-nucleus collisions, Nuclear Physics A **391**, 471–504 (1982). doi: 10.1016/0375-9474(82)90621-2.

[42] W. J. Światecki, K. Siwek-Wilczyńska, J. Wilczyński, et al., Fusion by diffusion. II. Synthesis of transfermium elements in cold fusion reactions, Phys. Rev. C **71**, 014602 (2005). doi: 10.1103/PhysRevC.71.014602.

[43] V. Zagrebaev, W. Greiner, Low-energy collisions of heavy nuclei: dynamics of sticking, mass transfer and fusion, Journal of Physics G: Nuclear and Particle Physics **34**, 1 (2006). doi: 10.1088/0954-3899/34/1/001.

[44] G.G. Adamian, N.V. Antonenko, W. Scheid, Model of competition between fusion and quasifission in reactions with heavy nuclei, Nuclear Physics A **618**, 176-198 (1997). doi: 10.1016/S0375-9474(97)88172-9.

[45] LI Jun-qing, ZUO Wei, FENG Zhao-qing, et al., Formation Mechanism of Super Heavy Nuclei in Heavy Ion Collisions, Nuclear Physics Review **23**, 396-398 (2006). doi: 10.11804/NuclPhysRev.23.04.396.

[46] W. Li, N. Wang, J. F. Li, et al., Fusion probability in heavy-ion collisions by a dinuclear-system model, Europhysics Letters **64**, 750 (2003). doi: 10.1209/epl/i2003-00622-0.

[47] S. E. Agbemava, A. V. Afanasjev, D. Ray, et al., Assessing theoretical uncertainties in fission barriers of superheavy nuclei, Phys. Rev. C **95**, 054324 (2017). doi: 10.1103/Phys-

RevC.95.054324.

[48] K. Hagino, N. Rowley, A. T. Kruppa, A program for coupled-channel calculations with all order couplings for heavy-ion fusion reactions, Computer Physics Communications **123**, 143-152 (1999). doi: 10.1016/S0010-4655(99)00243-X.

[49] Z.-Q. Feng, G.-M. Jin, F. Fu, et al., Production cross sections of superheavy nuclei based on dinuclear system model, Nuclear Physics A **771**, 50–67 (2006). doi: 10.1016/j.nuclphysa.2006.03.002.

[50] D. L. Hill, J. A. Wheeler, Nuclear Constitution and the Interpretation of Fission Phenomena, Phys. Rev. **89**, 1102–1145 (1953). doi: 10.1103/PhysRev.89.1102.

[51] V. I. Zagrebaev, Synthesis of superheavy nuclei: Nucleon collectivization as a mechanism for compound nucleus formation, Phys. Rev. C **64**, 034606 (2001). doi: 10.1103/PhysRevC.64.034606.

[52] X. J. Bao, Y. Gao, J. Q. Li, et al., Influence of nuclear basic data on the calculation of production cross sections of superheavy nuclei, Phys. Rev. C **92**, 014601 (2015). doi: 10.1103/PhysRevC.92.014601.

[53] C. Y. Wong, Interaction Barrier in Charged-Particle Nuclear Reactions, Phys. Rev. Lett. **31**, 766–769 (1973). doi: 10.1103/PhysRevLett.31.766.

[54] M. G. Itkis, G. N. Knyazheva, I. M. Itkis, et al., Experimental investigation of cross sections for the production of heavy and superheavy nuclei, Eur. Phys. J. A **58**, 178 (2022). doi: 10.1140/epja/s10050-022-00806-7.

[55] Yu. Ts. Oganessian, V. K. Utyonkov, D. Ibadullayev, et al., Investigation of ^{48}Ca-induced reactions with ^{242}Pu and ^{238}U targets at the JINR Superheavy Element Factory, Phys. Rev. C **106**, 024612 (2022). doi: 10.1103/PhysRevC.106.024612.

[56] Daiya Kaji, Kouji Morimoto, Hiromitsu Haba, et al., Decay Measurement of ^{283}Cn Produced in the ^{238}U(^{48}Ca, 3n) Reaction Using GARIS-II, J. Phys. Soc. Jpn. **86**, 085001 (2017). doi: 10.7566/JPSJ.86.085001.

[57] P. Möller, A.J. Sierk, T. Ichikawa, et al., Nuclear ground-state masses and deformations: FRDM(2012), Atomic Data and Nuclear Data Tables **109-110**, 1-204 (2016). doi: 10.1016/j.adt.2015.10.002.

[58] Yu. Ts. Oganessian, V. K. Utyonkov, M. V. Shumeiko, et al., Synthesis and decay properties of isotopes of element 110: ^{273}Ds and ^{275}Ds, Phys. Rev. C **109**, 054307 (2024). doi: 10.1103/PhysRevC.109.054307.